# Initial Rotor Position Detection in Synchronous Machines using Low Frequency Pulses

Simon Feuersänger, Mario Pacas
Universität Siegen, Germany
Simon.Feuersaenger@uni-siegen.de, jmpacas@ieee.org

***Abstract-*** **It is well-known that in the area of encoderless control methods for AC-drives a single approach is not capable to cover all speed ranges and all types of machines. Therefore, a combination of several methods is necessary. Especially in the case of electrically excited synchronous machines, the methods proposed for the low speed region and for the detection of the initial rotor position fail for many types of machines and demand for new solutions. In this paper, a method for the identification of the initial rotor position by injecting low frequency pulses is proposed. After the identification of the initial position, the drive is directly started with the help of a conventional high-speed method and rides through the critical speed region without any difficulties. The new method is designed for a reliable operation in a large group of electrically excited synchronous machines. Measurement results as well as a concept for the parameterization of the model are included in this paper.**

***Index Terms*** **—Sensorless control, permanent magnet machines, AC machines, brushless machines**

## I. Introduction

The control of any inverter fed AC-drive demands the information of the angular position of certain space phasors that describe the electrical machine. Depending on the particular control, either the position of one of the machine flux space phasors or the absolute rotor position is required. The use of a mechanical angular sensor in combination with an adequate machine model allows the calculation of every state variable in all imaginable operating points of the machine and thus the control of the drive. Unfortunately, a failure in the sensitive encoder directly leads to a costly downtime of the whole drive system.

For this reason, the improvement of the reliability of controlled AC-drives was the motivation of intensive research in the area of encoderless control. In order to fulfill the demand of an encoder independent control, certain machine models must provide the required angular positions just by evaluating the machine voltages and currents. The evaluation of the sensorless methods reported until now leads to the conclusion that a single approach is not capable to operate in the entire range of operating points [1]. In fact, most methods only work in a specified speed range. As a general rule, the encoderless techniques can be classified in several groups: Methods for the high speed region [1]-[3], methods for the low speed region [4]-[8], methods for the identification of the initial rotor position [2], [5]-[9] and methods for obtaining the speed and position when the inverter should connect to an already moving machine (flying start). It is obvious, that the exclusive use of a high-speed method does not always lead to a general solution and to a great improvement concerning reliability, as the drive is not able to start without an encoder. Consequently, a combination of several methods is required to cover the demands of a particular application.

All of the high-speed methods are based in principle on the evaluation of the induced stator voltage to detect the machine stator flux. These methods work on all AC-drives regardless of machine parameters. On the contrary, the low speed methods try to evaluate machine asymmetries by injecting adequate test signals in the stator winding. Thus, the applicability of these methods strongly depends on the machine characteristics and the use of such methods is consequently not possible for all machines. Comparable problems occur for identification concepts for the initial rotor position.

Almost all of the research effort in the field of encoderless control was dedicated to low voltage drives, or more precisely to induction machines (IM) and permanent magnet synchronous machines (PMSM). However, in high-power, medium-voltage applications, the selection criteria concerning the choice of the adequate machine type differ due to cost- and constructive issues. The typically used machines in those applications are induction machines for moderate power or electrically excited synchronous machines (EESM) for higher power. Permanent magnet machines are rarely used.

Although the encoderless methods for low voltage IMs work likewise with medium voltage IMs, the low-speed methods for PMSMs often fail when they are applied to EESMs. The reason is that these methods inject high frequency test signals in the stator winding in order to detect the difference of the machine mutual inductance in the direct- and quadrature axis [4]-[6]. At first glance, these methods seem to work excellent at least with salient pole EESMs as the difference in the mutual inductance is very high. However, in those machines the damper winding influences strongly the high frequency behavior of the machine. Accordingly, it is possible that the machine high frequency admittance is identical in both axes even in salient pole machines and thus the identification of the rotor position with these methods fail [10]. Unfortunately, this problem occurs in numerous EESMs and a continuous encoderless operation in the low speed region is not possible in these cases. However, a lot of applications do not demand a continuous operation in this particular speed range. In these cases, the drive only needs to pass through the low speed region during the acceleration from standstill. If the load torque during start up is not excessive, like in all pump or fan applications, the sensorless operation of the drive is still possible when the initial rotor position was identified correctly. The drive can switch directly to the high-speed method, accelerate and leave the critical low speed region.

978-1-4799-4033-2/14/$31.00 ©2014 IEEE

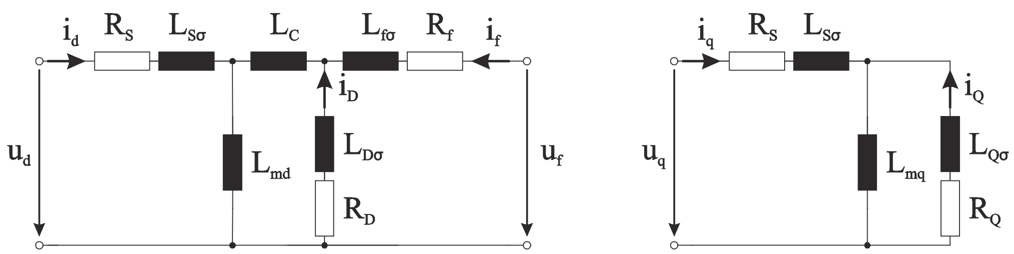


| | |
|---|---|
| $R_X$ | Winding resistance |
| $L_{X\sigma}$ | Stray inductance |
| $L_{mX}$ | Mutual inductance |
| $L_C$ | Canay inductance |

Index:

| | |
|---|---|
| S | Stator winding |
| d | d-axis stator winding |
| q | q-axis stator winding |
| f | Field winding |
| D | d-axis damper winding |
| Q | q-axis damper winding |

Fig. 1: Equivalent circuit in standstill in d- and q-axes of the SM

For all these reasons, the initial rotor position identification in EESMs is essential as it enables the use of encoderless control in many applications. However, the identification of the initial rotor position is not trivial. Even though there are several methods that evaluate different effects of the machine like the saturation state, different admittances in d- and q-axis, short circuit current when increasing the excitation, etc., all of them require special machine characteristics or cannot be applied in certain cases due to specific constraints. Moreover, there are many drives in which all known methods for the detection of the initial position fail and therefore an unrestricted encoderless control is not possible [11].

In order to fill this gap in encoderless methods for EESMs, a novel initial rotor position concept was presented in [11]. Meanwhile, this identification strategy was improved with new aspects and was validated through measurements. Now, this paper presents improvements as well as a novel approach to set the parameters of the identification method.

## II. Basic Idea

As a machine at stand-still is a purely passive system, it is necessary to inject test signals in order to get any information about the actual state of the machine. Hence, the question is what type of test signals should be injected and in which winding of the machine. The goal of the new identification concept is offering a solution for the initial rotor position detection for machines or applications where until now no method is applicable. Accordingly, the new procedure must base on a different physical effect than all prior proposals.

As already stated above, the nowadays standard approach is to inject high frequency signals in the stator winding (in this content "high frequency" signifies a frequency much higher than the nominal frequency. i.e. more than 200Hz). However, these methods fail at machines with same high frequency admittance caused by the damper winding.

The injection of test signals in the field winding is also problematically as this approach often fails in machines with brushless excitation. In this case, the overall electrical time constant of the field winding and excitation machine is too high to get a useful response in the stator winding [11]. Other approaches try to evaluate the saturation state of the machine but the damper winding often impedes the evaluation.

With the aim of finding an adequate test signal for the new method, the frequency response characteristic of several EESMs was examined according to their equivalent circuit as shown in Fig. 1 [12]-[13]. By assuming a sinusoidal voltage signal in the stator winding in d- or q- direction, the current response in the corresponding stator winding and finally the admittance ($Y_d=i_d/u_d$ and $Y_q=i_q/u_q$) is calculated. The field current controller also influences the reaction of the system. However, for a first approximation the field voltage is assumed to be constant (assuming low dynamics in the field controller). In fact, the absolute value of the admittance in both axes is not of great interest for the identification procedure; important is actually the difference between both admittances ($Y_d/Y_q$). Fig 2 shows the frequency dependency of this admittance ratio for different machines. In total, 14 machines for different applications and different power, voltage, frequency and speed ranges were investigated. All of them exhibit in general the same frequency characteristics like the ones shown in Fig 2 - namely, only slight differences in both admittances for higher frequencies but a distinctive difference for the low frequency range (generally between 1 and 10Hz). It is obvious, that even in those machines with similar high frequency admittances in both axes ($Y_d/Y_q \approx 1$) the rotor posi-

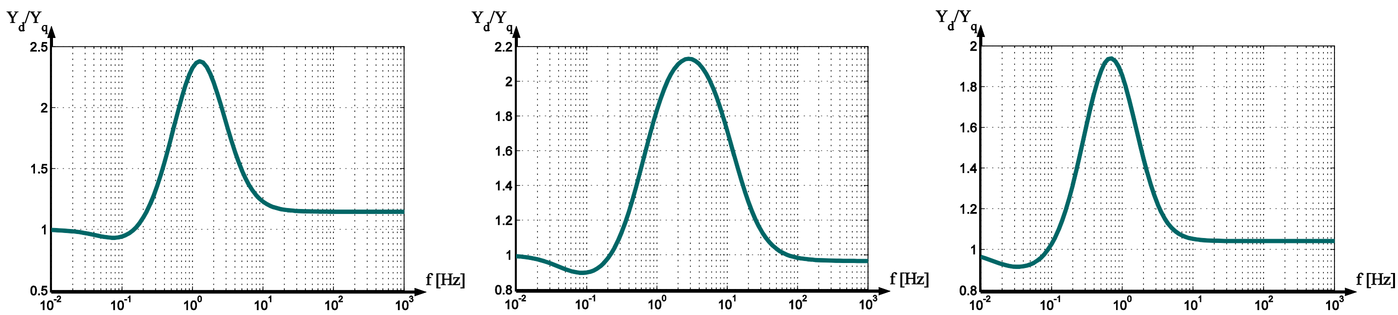


a) Cylindrical rotor, $P_N$=4,7MW, $n_N$=1500min-1, $p$=3 b) Salient pole, $P_N$=10MW, $n_N$=1800min-1, $p$=2 c) Salient pole, $P_N$=18MW, $n_N$=165min-1, $p$=6

Fig. 2: Frequency dependence of the admittance difference of several machines

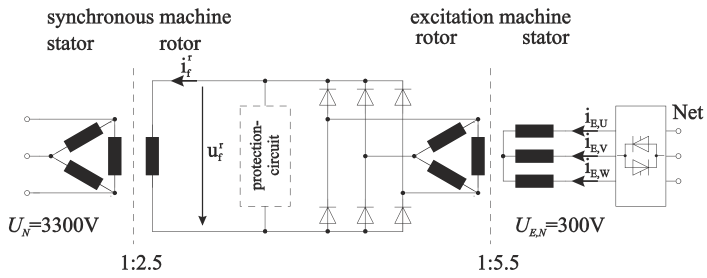


Fig. 3: Winding ratios of a brushless excited synchronous machine

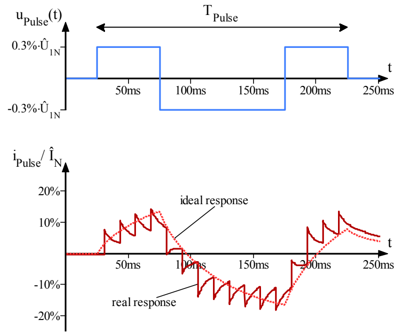


Fig. 4: Stator current response (simulation results)

tion can be easily identified if low frequency test pulses are injected.

In addition to this important fact, the use of low frequency signals offers another advantage: The evaluation of the test signal response in the field current becomes viable. As the sampling frequency of the field current is in general quite low (i.e. six times the net frequency, 300…360Hz), the measurement of the field current response is only possible for low frequency test signals. By injecting low frequency pulses in the stator winding, both, the current response in the stator winding as well as in the field winding, can be evaluated for the identification of the rotor position.

In brushless excited machines, the field current cannot be measured directly but can be reproduced from the three measured stator currents of the excitation machine [11].

It is important to point out that it is a great difference if a test signal, i.e. a voltage step, is injected in the field winding and the current response in the stator winding is measured or vice versa: the signal injection is carried out in the stator winding and the measurement in the field winding. As already stated above, methods, which are based on the first procedure, may fail, as the response in the stator winding is often too weak even if the maximum possible test signal amplitude is applied. In order to understand the different behavior in both cases, the winding ratios must be taken into account. Fig. 3 shows an example of the winding ratios in a brushless excited machine. As shown in the figure, the field winding of the synchronous machine exhibits a higher number of turns than the stator winding whereas the stator winding of the excitation machine has more number of turns than its rotor winding. Thus, the overall transfer ratio from the stator winding of the exciter to the main machine is the multiplication of both ratios and is in this case 13.75 (2.5·5.5). Unlike a conventional transformer, the winding with the highest number of turns exhibits the lowest nominal voltage. Accordingly, the injection of a voltage step with maximum amplitude on the exciter side leads to a magnetization of the machine comparable to those that is obtained by injecting a voltage step with an amplitude of solely 22V (300V/13.75) on the main side. As the nominal voltage of the main stator winding in this example is 3300V, it is obvious, that the response in the field winding is characteristic enough when a voltage pulse with adequate amplitude is injected in the main stator winding even if the injection in opposite direction does not have any notable effect.

As the admittance difference in the stator winding as well as the response in the field current are both effects which can be evaluated on almost every EESMs, it is expected that the new method can find application in numerous different EESMs. machines.

## III. Injection of Low Frequency Pulses

In order to identify the rotor position, several test signals have to be injected in different positions by the inverter. As the absolute machine admittance in the low frequency region is very large, voltage test pulses with an amplitude of about 5% the nominal machine voltage already lead to an excessive current response. Furthermore, in brushless excited machines the field current is always kept at a certain minimum level (e.g. 30% of its nominal value) to prevent damages of the rotating diodes during operation of the main inverter [11]. Hence, the machine is magnetized and can generate torque and thus perform unwanted motion during the identification process. To keep the motion of the drive at a certain acceptable minimum level (less than 5°), the voltage test amplitude needs to be very small. Typical values are 0.1% -2% of the machine nominal voltage.

A conventional space vector modulation is used to generate the voltage pulses. However, in a medium voltage inverter several conditions like minimum turn-on times of the semiconductors in the range of several ten microseconds must be respected. Thus, the only way to generate voltage pulses with such small amplitudes is to choose a very high modulation period. Furthermore, a rectangular voltage test signal is chosen as the inverter can replicate it best. Due to the large modulation period, the response in the stator current is distorted but includes all the required information for the rotor position identification. The test signal voltage $u_{Pulse}$ as well as the current response $i_{Pulse}$ in the stator winding are depicted in Fig 4. The signal $i_{Pulse}$ is the current component of the stator current space phasor $\underline{i}_1$ which lies in the same direction $\gamma_{Pulse}$ like the injected voltage pulse (2).

$$\underline{u}_{Pulse}(t) = u_{Pulse}(t) \cdot e^{j\gamma_{Pulse}} \tag{1}$$

$$i_{Pulse}(t) = \mathrm{Re}\left\{\underline{i}_1 \cdot e^{-j\gamma_{Pulse}}\right\} \tag{2}$$

$$\Delta\gamma = \gamma_{Pulse} - \gamma \tag{3}$$

If the voltage test pulse is now injected in the stator winding in different directions, the current response in the stator as

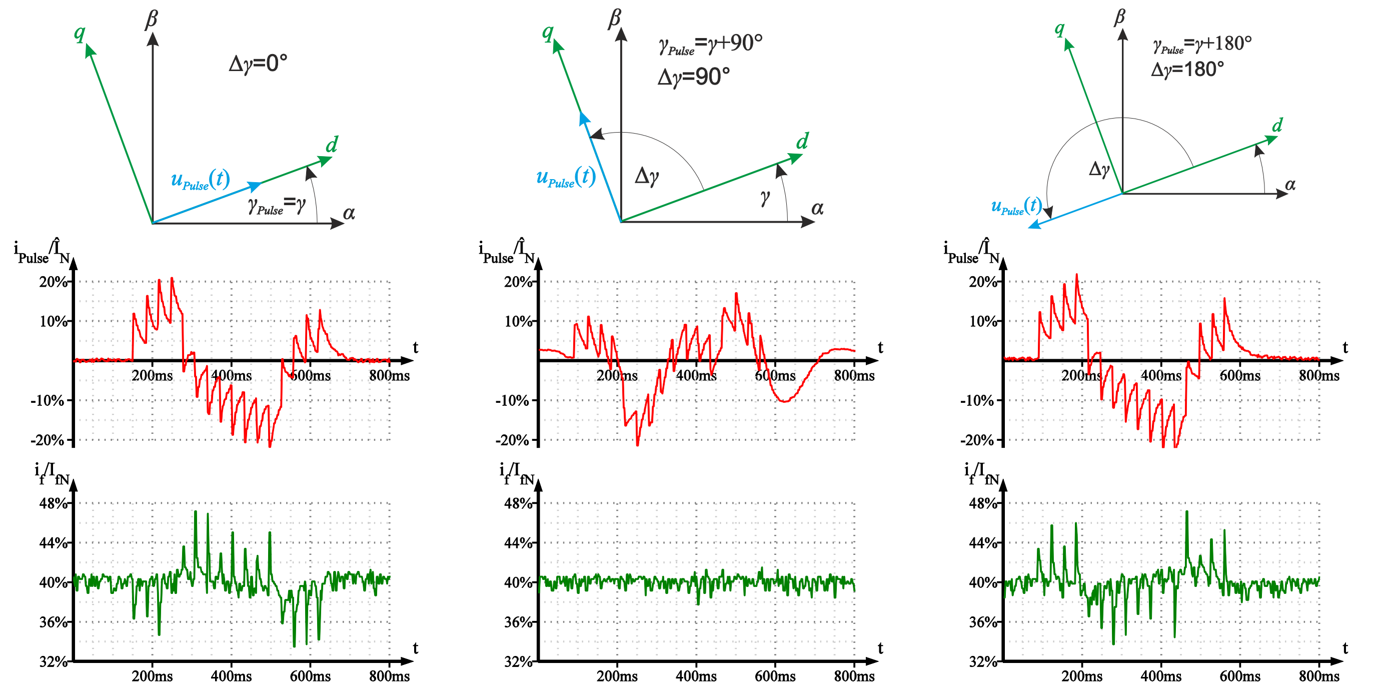


Fig. 5: Test pulse injection in different directions and their current responses (measurement results, 1.1MW Machine)

well as in the field current will vary depending on the angular difference $\Delta\gamma$ between injected voltage pulse $\gamma_{Pulse}$ and rotor position $\gamma$.

In Fig. 5 the measured current responses are shown, when injecting several pulses in different directions relative to the rotor position. As the admittance in the q-axis ($\Delta\gamma$=90°) of the machine is smaller than in the d-Axis ($\Delta\gamma$=0°), the stator current response in this direction is also lower. However, there is no difference between the stator current responses for a pulse injected in positive or negative d-axis, as the admittances are equal in both directions (pos. and neg. d-axis). Accordingly, the evaluation of the stator currents only permits the rotor position detection with an ambiguity of 180°. In contrast to this, the field current response shows a clear difference in such cases and thus allows the identification of the rotor position without ambiguity.

For the automatically evaluation of different current responses, quantities, which summarize all the important information of the transient current responses into just one value are necessary. These quantities are called “indicators” and can be calculated as follows:

$$\Lambda_s = \frac{1}{T_{Pulse}} \int_0^{T_{Pulse}} \frac{i_{Pulse}(t)}{\hat{I}_N} \cdot \cos(\omega_{Pulse} t) dt \tag{4}$$

$$\Lambda_f = \frac{1}{T_{Pulse}} \int_0^{T_{Pulse}} \frac{i_f(t)}{\hat{I}_N} \cdot \cos(\omega_{Pulse} t) dt \tag{5}$$

$$\omega_{Pulse} = \frac{2\pi}{T_{Pulse}} \tag{6}$$

The calculation of the stator indicator $\Lambda_s$ as well as of the field indicator $\Lambda_f$ is based on the calculation of the first harmonic of the Fourier series that describe $i_{Pulse}$ respectively $i_f$, by assuming $T_{Pulse}$ as the period of the fundamental. However, an even distribution is supposed and only the cosine coefficients are used.

Both indicators, the stator indicator $\Lambda_s$ and the field indicator $\Lambda_f$, are calculated for each injected voltage pulse. Now, the angular dependency of these indicators is interesting. For this reason, an identification run (ID-run) is executed at standstill for test purposes in which several voltage pulses are injected in steps of 15° to each other and the corresponding indicators are measured. Fig. 6 presents the results of such an ID-run for different test signal parameters. The measured rotor position $\gamma_{measured}$ is shown as reference. Especially in Fig. 6a) and c) the general characteristic of the indicator curves can be seen: The stator indicator exhibit its maximum values if the pulse is injected in positive or negative d-axis whereas the field current indicator has its minimum value at positive d-axis ($\gamma_{Pulse}=\gamma_{measured}$) but its maximum value at negative d-axis ($\gamma_{Pulse}=\gamma_{measured}+180°$). Depending on the test signal parameters, especially the test signal frequency, the indicator curves vary strongly: The indicators are mainly affected by the admittances in d- and q- axis. The dynamics of the field controller has also big influence on the results, can even compensate the effect in the field winding and a backward calculation that considers the dynamics of the controller is not practicable. Fig. 6b) shows as an example the results for a test signal, which should not be used for the identification because it leads to a highly distorted field indicator. For all these reasons, suitable test signals are necessary for high-quality indicator curves.

## IV. Identification Strategy

The above-explained ID-Run is not suitable during a normal start-up, as too many pulses need to be injected, which is time consuming, especially for very low frequencies. Thus, the

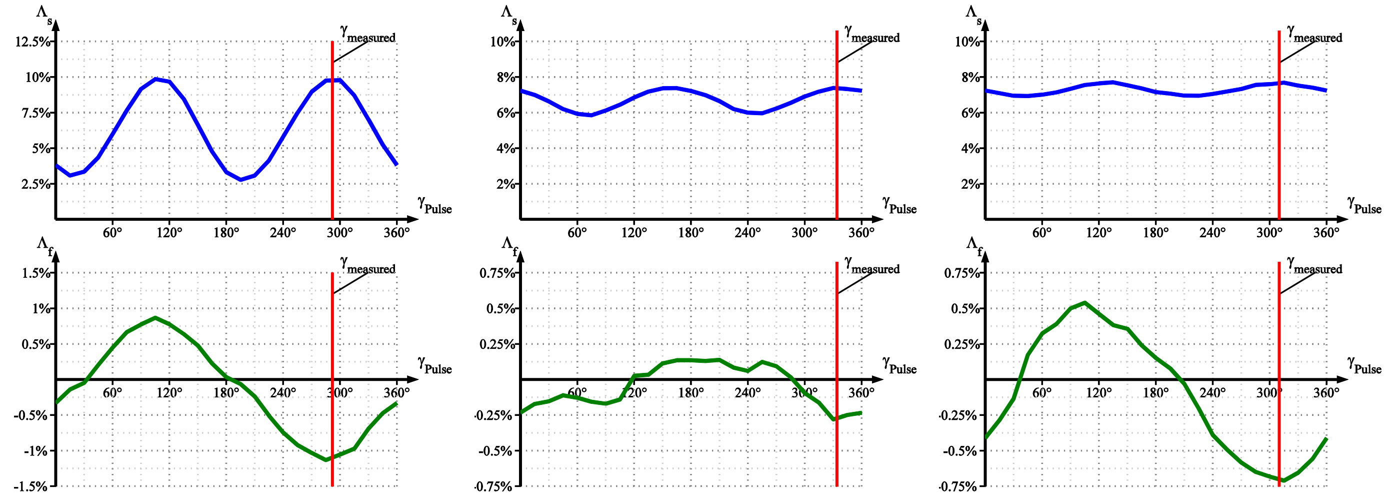


a) $f_{Pulse}$=2Hz, $\hat{u}_{Pulse}$=1%$\cdot\hat{U}_{1N}$ b) $f_{Pulse}$=5Hz, $\hat{u}_{Pulse}$=1%$\cdot\hat{U}_{1N}$ c) $f_{Pulse}$=10Hz, $\hat{u}_{Pulse}$=2%$\cdot\hat{U}_{1N}$

Fig. 6: ID-run with different test signal parameters. (measurement results, 1.1MW Machine, brushless excitation)

main goal is to inject only few pulses in order to detect the angles where the stator indicator $\Lambda_s$ exhibits one of its maximum values or where the field indicator $\Lambda_f$ exhibits its minimum value.

The strategy proposed here interpolates the whole indicator curves with the Fourier-series by measuring the indicators only at either three or six positions.

In general, Fourier series can describe every periodical signal. Hence, the corresponding Fourier-coefficients of harmonic "ν" for the stator indicator are obtained by following equations, regarding 360° of the electrical angle as fundamental period:

$$\alpha_{s\nu} = \frac{1}{\pi}\int_0^{2\pi} \Lambda_s(\gamma_{Pulse})\cdot\cos(\nu\cdot\gamma_{Pulse})d\gamma_{Pulse} \tag{7}$$

$$\beta_{s\nu} = \frac{1}{\pi}\int_0^{2\pi} \Lambda_s(\gamma_{Pulse})\cdot\sin(\nu\cdot\gamma_{Pulse})d\gamma_{Pulse} \tag{8}$$

However, each ideal indicator curve exhibits only one harmonic: The field indicator only contains the fundamental wave ($\alpha_{f1}$, $\beta_{f1}$), whereas the stator indicator only consists of the 2nd harmonic ($\alpha_{s2}$, $\beta_{s2}$) and an offset ($\Lambda_{s,avg}$). Hence, the two indicator curves can be approximated with the following formulas:

$$\Lambda_s(\gamma_{Pulse}) = \Lambda_{s,avg} + \alpha_{s2}\cdot\cos(2\gamma_{Pulse}) + \beta_{s2}\cdot\sin(2\gamma_{Pulse}) \tag{9}$$

$$\Lambda_f(\gamma_{Pulse}) = \alpha_{f1}\cdot\cos(\gamma_{Pulse}) + \beta_{f1}\cdot\sin(\gamma_{Pulse}) \tag{10}$$

As the coefficients are obtained by a finite number $n$ of measurements, the calculation of the coefficients is as follows:

$$\alpha_{s2} = \frac{1}{n}\sum_{k=0}^{n-1} \Lambda_s(\gamma_{Pulse,k})\cdot\cos(2\cdot\gamma_{Pulse,k}) \tag{11}$$

$$\beta_{s2} = \frac{1}{n}\sum_{k=0}^{n-1} \Lambda_s(\gamma_{Pulse,k})\cdot\sin(2\cdot\gamma_{Pulse,k}) \tag{12}$$

$$\alpha_{f1} = \frac{1}{n}\sum_{k=0}^{n-1} \Lambda_f(\gamma_{Pulse,k})\cdot\cos(\gamma_{Pulse,k}) \tag{13}$$

$$\beta_{f1} = \frac{1}{n}\sum_{k=0}^{n-1} \Lambda_f(\gamma_{Pulse,k})\cdot\sin(\gamma_{Pulse,k}) \tag{14}$$

$$\gamma_{Pulse,k} = k\cdot\Delta\gamma_{Pulse,}\; k = 0,1,2,...,n \tag{15}$$

$\gamma_{Pulse,k}$ is the angle of the injected voltage pulse, respectively the angle at which the two indicators are measured. The voltage pulses are injected in constant angular steps of $\Delta\gamma_{Pulse}$=60° in the stator winding. With these steps, the inverter always injects one of its "natural" space phasors, which leads to the highest accuracy of the identification method.

In order to cover the complete angular range of 360°, $n$=6 pulses need to be injected. However, due to the symmetry in both indicators (16)(17), the integration over the reduced angular range of 180° is sufficient for the calculation of the corresponding coefficients.

$$\Lambda_s(\gamma_{Pulse}) = \Lambda_s(\gamma_{Pulse}+\pi) \tag{16}$$

$$\Lambda_f(\gamma_{Pulse}) = -\Lambda_f(\gamma_{Pulse}+\pi) \tag{17}$$

Thus, the number of pulses can be chosen to be either $n$=3 or $n$=6. Now the indicator curves can be interpolated by injecting only a few pulses in the stator winding. Fig. 7 shows the interpolated curves compared to the measured curves during the ID-run. The identified angular values at maximum stator indicator ($\gamma_{is,a}$, $\gamma_{is,b}$) or minimum field indicator ($\gamma_{if}$) are shown as well. These angular values can be easily calculated based on the identified Fourier-coefficients by following equations:

$$\gamma_{is,a} = \frac{1}{2}\arctan 2(\beta_{s2},\alpha_{s2}) \tag{18}$$

$$\gamma_{is,b} = \gamma_{is,a} + \pi \tag{19}$$

$$\gamma_{if} = \arctan 2(\beta_{f1},\alpha_{f1}) + \pi \tag{20}$$

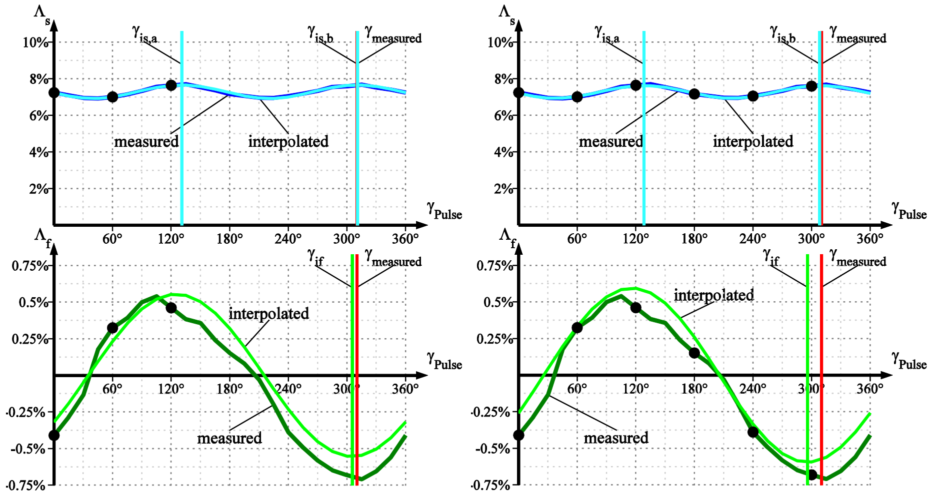


a) Interpolation with $n$=3 injected pulses b) Interpolation with $n$=6 injected pulses

Fig. 7: Interpolated indicator curves in comparison with the measured curves during the ID-run

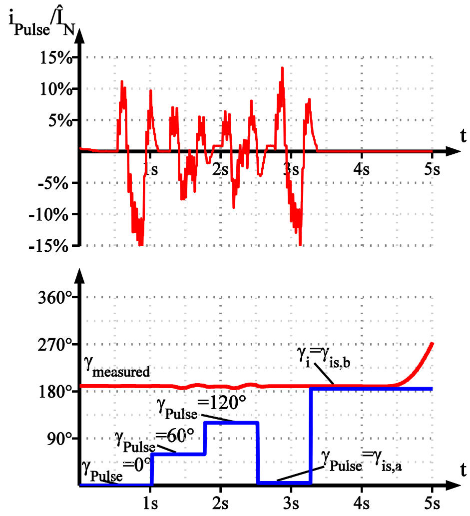


Fig. 8:Start up procedure with Method "b" and n=3

Now, two different strategies to detect the rotor position are possible:

a) Field indicator method

The first method uses the identified angle at minimum field indicator $\gamma_{if}$ as identified shaft position ($\gamma_i$=$\gamma_{if}$). Thus, the identification bases purely on the evaluation of the field current but the stator indicator is not used at all. However, in some machines, especially brushless excited machines, in which the field current is not measured directly but reconstructed, the quality of the field indicator curve and finally the precision of the identification, are not satisfying. In these cases, the second strategy is preferable.

b) Combined method

The rotor position detection by using only the stator indicator is not possible as the position can only be identified with 180°-ambiguity. However, when combining both indicators the high accuracy of the stator indicator as well as the elimination of the ambiguity are achieved: The two possible rotor positions ($\gamma_{is,a}$, $\gamma_{is,b}$) are first calculated based on the stator indicator (18)(19). In a next step, a further pulse is injected in the position of the first identified angle $\gamma_{is,a}$ and the sign of the field indicator $\Lambda_f$ is examined. If the field indicator at this position is negative, the d-axis lies at this position ($\gamma_i$=$\gamma_{is,a}$) whereas a positive sign means that the pulse was injected in the negative d-axis. Thus, the identified rotor position is $\gamma_i$=$\gamma_{is,b}$. Fig. 8 shows the start-up procedure using this method to identify the rotor position and the high-speed method to accelerate.

## V. EXPERIMENTAL RESULTS AND SETTING OF PARAMETERS

Measurements on a 1.1MW medium voltage synchronous machine with a three level inverter were performed. The machine is a special machine built for laboratory tests and contains two different excitation systems: either direct excitation or brushless excitation. As the control parameters for the two excitation systems vary, the performance of the proposed method also varies depending on which excitation method is used. Table 1 shows the maximum error of the identified electrical rotor position occurred during several measurements depending on the test signal frequency and identification method.

It is obvious, that the choice of adequate test signal parameters, especially the test signal frequency, is essential for a satisfactory performance. With well-chosen parameters, the rotor position can be identified with an error of less than 5°, which ensures the correct start-up of the drive. However, improper parameters lead to unusable performance.

As the accuracy of the procedure depends on many different aspects like field controller, saturation behavior, machine parameters, etc. it is hard to calculate the best test signal parameters offline and an automatically setting of the parameters during commissioning of the drive is therefore desirable.

By comparing the results in Table 1 with the indicator curves during ID-run (partially shown in Fig. 6), it is noticeable that a high-quality indicator curve leads to good results but a distorted curve to high errors.

Hence, it is reasonable to analyze and compare the quality of the resulting indicator curves during ID-run. Two criteria of the indicator curves are examined: the THD-value (**T**otal **H**armonic **D**istortion) and the quotient between fundamental wave and average value.

For the calculation of the THD of the field indicator curve ($THD_{\Lambda f}$) the corresponding harmonics $\Lambda_{f\nu}$ are first calculated according to (21) and (7)-(15). During the ID-run, $n$=24 voltage pulses are injected in angle steps of $\Delta\gamma_{Pulse}$=15° to each other. Thus, the harmonic contents above the 12$^{th}$ harmonic (24/2) cannot be calculated. The THD of the field indicator is then calculated by (22). The calculation of the stator indicators THD is equivalent, considering its double frequency of the fundamental wave.

$$\Lambda_{f\nu} = \sqrt{\alpha_{f\nu}^2 + \beta_{f\nu}^2} \tag{21}$$

$$THD_{\Lambda f} = \sqrt{\frac{\Lambda_{f2}^2 + \Lambda_{f2}^2 + \Lambda_{f2}^2 + ... + \Lambda_{f12}^2}{\Lambda_{f1}^2}} \tag{22}$$

Finally, for each of the two identification methods a) and b) a cost function is defined ($C_a$, $C_b$), which allows the conclusion about the applicability of the corresponding method. A higher value signifies less applicable and a value greater than 1.0 excludes the corresponding method for the rotor position identification.

$$C_a = THD^2_{\Lambda f} \cdot g_{THDf} + \left( \frac{\overline{\Lambda_f}}{\Lambda_{f1}} \right) g_{avg,\mathrm{f}} + \frac{T_{Pulse}}{1s} g_T + C_{brushless} \quad (23)$$

$$C_b = THD^2_{\Lambda S} \cdot g_{THDS} + \left( \frac{\overline{\Lambda_S}}{\Lambda_{S2}} - 1 \right) g_{avg,\mathrm{S}} + \frac{T_{Pulse}}{1s} g_T + C_{\min,f} \quad (24)$$

Besides the THD- and average values ($\overline{\Lambda_f}$, $\overline{\Lambda_S}$), also the test signal period $T_{Pulse}$ is included in the cost function as higher frequencies are preferable due to shorter identification time and less motion of the machine shaft during the test signal injection.

Method a) bases solely on the evaluation of the field indicator and thus does not contain information about the stator indicator. However, a heuristic factor "$C_{brushless}$" is included which is set to 0.15 in case of brushless excitation, or to zero for direct excitation. In that manner, method b) which combines both indicators is preferred in brushless excited machines. In contrast, method b) primary bases on the stator indicator but also needs a minimum quality of the field indicator curve to eliminate the 180°-ambiguity. In this case the factor "$C_{min,f}$" is set to 1.0 if the cost function for method a) is greater than 1.5, or set to zero if not. Hence, method b) is only chosen, if the quality of the field indicator reaches a minimum level. Table 1 contains the values of the cost-functions for different test signal parameters. The corresponding empirically obtained gains $g_{THDf}$, $g_{THDS}$, $g_{avg,f}$, $g_{avg,S}$ and $g_T$ are depicted in Table 2.

The best cost function for direct excitation is achieved with method a) and a pulse frequency of 10Hz. For brushless excitation method b) and a test signal frequency of 2Hz should be chosen. Both cases ensure an error of less than 5° electrically of the identification procedure at this machine.

Table 1: Accuracy of the identification method using 3 Pulses and cost functions for different test signal parameters

| | Method a) | | Method b) | |
|---|---|---|---|---|
| Direct excitation | $\gamma_{error}$* | $C_a$ | $\gamma_{error}$* | $C_b$ |
| $f_{Pulse}$= 2Hz | 31° | 1.24 | 4,3° | .10 |
| 5Hz | 2,2° | .19 | 10° | .55 |
| 10Hz | 4,1° | **.031** | 10,7° | .47 |
| Brushless excitation | | | | |
| $f_{Pulse}$=1Hz | 84° | 4.99 | 3,4° | 1.11*[2] |
| 2Hz | 10,7° | .70 | 4,9° | **.076** |
| 5Hz | 60° | 1.98 | 18° | 1.27*[2] |
| 10Hz | 13° | .70 | 14,8° | .58 |

* electrical angle. (Four pol pairs)
*[2] quality of field indicator insufficient

Table 2: Cost function gains

| | | | | | |
|---|---|---|---|---|---|
| $g_{THDf}$ | 5 | $g_{THDS}$ | 5 | $g_T$ | 0.1 |
| $g_{avg,f}$ | 20 | $g_{avg,S}$ | 0.025 | | |

## VI. CONCLUSION

A novel identification method for the initial rotor position in electrically excited synchronous machines was proposed. It injects low frequency voltage pulses in several directions in the stator winding and evaluates the stator current and field current response. Yet the accuracy of the procedure depends strongly on the test signal parameters. These parameters can be chosen automatically during the commissioning of the drive by evaluating the quality of the current responses. With the identified initial rotor position, the drive can start without encoder and accelerate to a speed in which an encoderless method works and continues the operation.

## APPENDIX

### A. Machine data:

| | | | | | |
|---|---|---|---|---|---|
| $P_N$ | 1.1MW | $n_N$ | 225min$^{-1}$ | $f_N$ | 15Hz |
| $U_N$ | 3300V | $I_N$ | 186A | $p$ | 4 |

### B. Inverter data:

| | | | |
|---|---|---|---|
| $S_N$ | 3MVA | Topology | 3-Level NPC inverter with IGCTs |
| $U_{dc}$ | 4670V | $I$-measurement | 10Bit, Range: ±1228A |

## REFERENCES


[1] Pacas, M.; "Sensorless Drives in Industrial Applications", Industrial Electronics Magazine, IEEE vol. 5, no. 2, pp.16-23, June 2011

[2] Niemelä, M.; "Position Sensorless Electrically Excited Synchronous Motor Drive for Industrial Use Based on Direct Flux Linkage and Torque Control", Ph.D. dissertation, Lappeenranta University of Technology, Lappeenranta, Finland, 1999

[3] Holtz, J.; "Speed estimation and sensorless control of AC drives", Industrial Electronics, Control and Instrumentation, 1993. Proceedings of the IECON '93. International Conference on, pp.649-654 vol.2, Nov 1993

[4] Linke, M.; Kennel, R.; Holtz, J.: "Sensorless speed and position control of synchronous machines using alternating carrier injection", Electric Machines and Drives Conference, 2003. IEMDC'03. IEEE International, vol.2, pp. 1211- 1217 vol. 2, 1-4 June 2003

[5] Holtz, J.; "Initial Rotor Polarity Detection and Sensorless Control of PM Synchronous Machines", Industry Applications Conference, 2006. 41st IAS Annual Meeting. Conference Record of the 2006 IEEE. , vol.4, no., pp.2040-2047, 8-12 Oct. 2006

[6] Schroedl, M.; "Sensorless control of AC machines at low speed and standstill based on the "INFORM" method", Industry Applications Conference, 1996. 31. IAS Annual Meeting, IAS '96., Conference Record of the 1996 IEEE, vol.1, pp.270-277 vol.1, Oct 1996

[7] Alaküla, M.; "On the Control of Saturated Synchronous Machines", Ph.D. dissertation, Dept. IEA, Lund Institute of Technology, Lund, Sweden, 1993

[8] Uzel, David; Peroutka, Zdenek, "Resolver motivated sensorless rotor position estimation of wound rotor synchronous motors", Industrial Electronics (ISIE), 2013 IEEE International Symposium on, pp.1,6, May 2013

[9] Parasiliti, F.; Petrella, R.; Tursini, M.; "Initial rotor position estimation method for PM motors" Industry Applications, IEEE Transactions on , vol.39, no.6, pp.1630,1640, Nov.-Dec. 2003

[10] Feuersänger, S.; Pacas, M.; "Initial Rotor Position Detection in Electrically Excited Medium Voltage Synchronous Machines", PCIM 2012, Nürnberg, Germany, 08-10 May 2012

[11] Feuersänger, S.; Pacas, M., "Initial rotor position identification in medium voltage synchronous machines", IECON 2012 - 38th Annual Conference on, pp.1852,1857, Oct. 2012

[12] Canay, I.M.; "Causes of Discrepancies on Calculation of Rotor Quantities and Exact Equivalent Diagrams of the Synchronous Machine", Power Apparatus and Systems, IEEE Transactions on vol. PAS-88, no.7, pp.1114-1120, July 1969

[13] Kaukonen, J.; "Salient Pole Synchronous Machine Modelling in an Industrial Direct Torque Controlled Drive Application", Ph.D. dissertation, Lappeenranta University of Technology, Lappeenranta, Finland, 1999